



Spring 2021

Multifunctional Polymer-Nanoparticle Composites for Surface-Enhanced Raman Scattering Applications

Aliandra E. Pierce
Western Washington University

Samantha A. Patrick
Western Washington University

Steven R. Emory
Western Washington University

Follow this and additional works at: https://cedar.wwu.edu/wwu_honors

 Part of the [Chemistry Commons](#)

Recommended Citation

Pierce, Aliandra E.; Patrick, Samantha A.; and Emory, Steven R., "Multifunctional Polymer-Nanoparticle Composites for Surface-Enhanced Raman Scattering Applications" (2021). *WWU Honors College Senior Projects*. 489.

https://cedar.wwu.edu/wwu_honors/489

This Project is brought to you for free and open access by the WWU Graduate and Undergraduate Scholarship at Western CEDAR. It has been accepted for inclusion in WWU Honors College Senior Projects by an authorized administrator of Western CEDAR. For more information, please contact westerncedar@wwu.edu.

Multifunctional Polymer-Nanoparticle Composites for Surface-Enhanced Raman Scattering Applications

Aliandra E. Pierce, Samantha A. Patrick, Steven R. Emory
Western Washington University Department of Chemistry
Honors Thesis

Abstract.

To create a multifunctional nanoparticle-based optical sensor, a pH-responsive microgel consisting of 20% polystyrene (PS) and 80% poly(2-vinylpyridine) (P2VP) surface-coated with gold nanoparticle (NP) seeds was synthesized. The pH-responsive microgel serves as a size-tunable scaffold for the assembly of the surface-enhanced Raman scatter active (SERS-active) metal, gold. The random copolymer of PS and P2VP (PS₂₀P2VP₈₀) is sterically stabilized by poly(ethyleneglycol) methyl ether methacrylate (PEGMA) and lightly crosslinked with divinylbenzene (DVB) to allow for reversible pH-swelling over multiple cycles of acid-base titration. The ability to swell and de-swell in response to changes in pH allows for the tuning of gold NP interparticle distance, consequently affecting the SERS activity. The gold NPs adsorbed to the surface of the microgels dramatically enhances the SERS spectroscopy signals depending on their size and spacing. Attempts to encapsulate magnetic NPs were accomplished and would allow for the extraction of microgels from a sample matrix through applying an external magnetic force. These NP-microgel composites are synthesized, characterized, and their SERS-activity is demonstrated.

1. Introduction

The Emory and Rider research groups at Western Washington University have been working collaboratively to develop a polymer-based system for surface-enhanced Raman scattering (SERS) spectroscopy applications. Previous work by these groups has demonstrated the synthesis of a random copolymer consisting of 20% polystyrene and 80% 2-vinylpyridine (PS₂₀P2VP₈₀) lightly crosslinked with DVB, a polymer ratio that is optimal for forming stable micrometer-sized beads.¹ The average microgel bead diameter of ~275 nm is suitable for future biological imaging applications.² Cellular systems are on the micrometer to nanometer length scale, thus the synthesis of structures on this length scale or below is essential for the development of new optical probes for biological systems.²

Surface-enhanced Raman scattering (SERS) is a highly sensitive spectroscopic technique that can be used to identify molecules when adsorbed to the surface of metallic nanoparticles (NPs) such as gold or silver.³ New imaging methods are sought after by scientists in order to help them study a range of problems such as brain function, cancer detection, and quantification of environmental contaminants. Nanostructures are currently being utilized for drug delivery, labeling agents, sensors, and the enhancement of electromagnetic fields.² The SERS effect arises most dominantly from the uniform oscillations of conduction band electrons in the metallic NPs that give rise to localized surface plasmon resonances (LSPR). These LSPR oscillate in resonance with the applied electric field of light, enhancing the SERS spectroscopy signal. This electric field amplification increases the SERS signal by many orders of magnitude, making metal NPs, and specifically gold NPs, a desirable candidate for optical sensors.

Encapsulating magnetic NPs (Fe₃O₄, magnetite, SPIONs) within the PS₂₀P2VP₈₀ microgel beads would create a multifunctional microgel with the properties of both materials. Superparamagnetic

iron(II,III) oxide nanoparticles (SPIONs) encapsulated within a microgel bead theoretically have the unique magnetic, thermal, optical, and electronic properties of magnetic nanoparticles, as well as the chemical and physical properties of a polymer matrix (e.g. SERS activity and pH-swelling).⁴ Introducing magnetic properties enables active manipulation of the microgel beads in complex systems. For example, the beads could be extracted from environmental samples or guided towards specific cellular regions using magnetic fields. The ability to enrich or direct the microgel beads would allow lower concentrations of the particles to be used, and thus improve detection sensitivity.

The project goal is to develop a synthetic route of creating multifunctional microgel beads for optical sensing/imaging. To achieve this task, gold NPs will be electrostatically loaded onto the surface of the microgels; previous work in the Emory Group demonstrated this process.¹ By coating the microgel beads with gold NPs, the microgel beads become SERS-active. Encapsulation of SPIONs inside polymer microgel beads was attempted using the established emulsion polymerization procedure to theoretically produce magnetic polymer microgel beads. Further research into this encapsulation method must be done in the future before adsorbing and growing AuNPs on the surface of the magnetic-polymeric substrate.

2. Methods

2.1. PS₂₀P2VP₈₀ Microgel Synthesis

Styrene (PS, 99%, stabilized; Acros), 2-vinylpyridine (P2VP, 97%, stabilized; Acros), and divinylbenzene (DVB, 55%; Aldrich) were purified through columns packed with glass wool and aluminum oxide to remove inhibitor molecules present within the stock solution that prevent auto-polymerization. The purified monomers were collected in 20 mL scintillation vials and set aside

for later. The emulsion polymerization was carried out within a 100 mL Schlenk flask attached to a Schlenk line under a N₂ atmosphere. Before purging the flask, the Aliquat 336 surfactant (0.30 g) and a stir bar were added. PEGMA stabilizer (0.45 g) was dissolved in 10 mL Ultrapure water within a 20 mL scintillation vial before its addition to the Schlenk flask. In the same PEGMA vial, 15 mL portions of Ultrapure water were added two times (for a total of 40 mL H₂O) to aid in the transfer of PEGMA to the reaction flask. The flask was capped with a septum and cycled onto the Schlenk line three times over a period of 15 minutes. After purging the headspace of the Schlenk flask, it was lowered into a 70 °C oil bath while stirring at a rate of approximately 350 rpm. A 20 mL scintillation vial was capped with a septum and a dual needle system was used to purge the flask with N₂ for 15 minutes. The monomers PS (1.00 mL), P2VP (4.00 mL), and DVB (0.03 mL) were injected into the purged scintillation flask using appropriately-sized syringes and needles. After swirling the scintillation flask a few times to gently mix the monomers, the monomer solution was transferred into the heated reaction flask. An external temperature probe was used to note when the oil bath rose back to its initial temperature of 70 °C and the contents of the flask appeared homogeneous (no oil droplets on the surface of the solution). An initiator solution containing the water-soluble 2,2'-azobis(2-methylpropionamidine) dihydrochloride (AIBA) (0.05311 g) was created by dissolving the initiator in 5.00 mL Ultrapure water. This solution was injected into the reaction flask, which stirred for 21 h at 70 °C under a N₂ atmosphere. The resulting microgels were purified three times using an ultracentrifuge set to 10,000 rpm for 10 min each. After each centrifugation, the impurities in the top layer were decanted off and the microgels were resuspended in ultrapure water.

2.2. *AuNP Seed-PS₂₀P2VP₈₀ Synthesis*

In a 50 mL beaker, the previously synthesized PS₂₀P2VP₈₀ microgels (1.00 mL) were diluted in Ultrapure water (5.00 mL). A solution of potassium tetrachloroaurate(III) (98%; Acros) (17.5 mL, 20 mM) was created and mixed with the contents of the beaker for 1 h. The resulting solution was transferred into dialysis tubing and purified in Ultrapure water for 48 h. The dialysis bath water was changed every 8-12 h. After 48 h of purification, the solution was removed from the bath and an aliquot (1.00 mL) was transferred to a 25 mL beaker. A solution of dimethylamine borane complex (DMAB) (55%; Sigma-Aldrich) (5.00 mL, 10 mM) was freshly-made and added to the beaker at a rate of 150 mL/s. The resulting solution stirred for 1 h before being transferred to dialysis tubing and placed in a dialysis bath for 24 h. The bath water was changed every 8-12 h.

2.3. *Au@AuNP-PS₂₀P2VP₈₀ Microgel Synthesis*

An aliquot of the resulting AuNP Seed-PS₂₀P2VP₈₀ microgels (1.00 mL) was diluted in Ultrapure water (13.00 mL). This solution was mixed with sodium citrate (dihydrate, Mallinckrodt Chemicals) (250 μ L, 38.8 mM) for 4 minutes before the dropwise addition of potassium tetrachloroaurate(III) (230 μ L, 25 mM). The resulting solution stirred for 8 min before hydroxylamine hydrochloride (J.T. Baker) (340 μ L, 10 mM) was added at a rate of 10 drops per second. The solution stirred for 1 h and was purified through centrifugation for 15 min at 5,000 rpm.

2.4. Fe_3O_4 - $PS_{20}P2VP_{80}$ Microgel Synthesis

SPIONs were synthesized following a procedure by Xu *et al.*⁵ The SPIONs (0.37 g) were dissolved in the surfactant solution via sonication bath for 45 m. The surfactant solution was created using sodium dodecyl sulfate (SDS) (0.214 g) in 8 mL Ultrapure water. The $PS_{20}P2VP_{80}$ Microgel Synthesis procedure was followed using the magnetite-SDS solution as the surfactant rather than Aliquat 336. The 8 mL of Ultrapure water used to make the SDS solution was subtracted from the total volume of water used to transfer PEGMA to the reaction flask, for a 32 mL addition of Ultrapure water rather than the 40 mL total volume of water described in $PS_{20}P2VP_{80}$ Microgel Synthesis.

2.5. AuNP-loaded Fe_3O_4 - $PS_{20}P2VP_{80}$ Microgel Synthesis

The AuNP-loaded $PS_{20}P2VP_{80}$ Synthesis was followed using a 1.00 mL aliquot of Fe_3O_4 - $PS_{20}P2VP_{80}$ microgels in the place of non-magnetic microgels.

2.6. Characterization

UV-Vis Spectroscopy. UV-Vis extinction spectra were acquired using a diode array UV-Vis spectrophotometer (Jasco V-670) and 10.00 mm polystyrene cells (Fisher). The AuNP- $PS_{20}P2VP_{80}$ microgels were diluted by a factor of 10 before collecting data.

Atomic force microscopy (AFM). AFM data were collected on a low-power microscope stage (TS-300/LT) with a Nikon Eclipse Ti-U camera attachment. Images were acquired using tapping mode with a scan rate of 1.00 Hz, 512 samples per line, and the ScanAsyst Auto Control settings

activated. Samples were prepared by allowing a 10 μL aliquot to dry on a coverslip, which was then taped to a microscope slide before placing it in the instrument.

Scanning transmission electron microscopy (STEM). STEM data were collected on a JEOL Field Emission scanning electron microscope (JEOL SM-13020RLV). Sample preparation consisted of dropping a 2-5 μL aliquot onto a carbon 300 mesh copper TEM grid (Formvar) and allowing it to dry before STEM imaging.

Energy-dispersive x-ray spectroscopy (EDS). EDS data were collected on a JEOL Field Emission scanning electron microscope (JEOL SM-13020RLV). Sample preparation consisted of dropping a 2-5 μL aliquot onto a carbon 300 mesh copper TEM grid (Formvar) and allowing it to dry before EDS analysis.

Raman microscopy. Raman scattering data were collected on a Renishaw inVia confocal Raman microscope using the x50 L objective lens and a 633 nm He-Ne laser source. A Renishaw Centrus 2NA004 detector was used. For image mapping, the scan type was set to static, the exposure time was 0.500 s, and one accumulation was acquired.

3. Results and Discussion.

The $\text{PS}_{20}\text{P2VP}_{80}$ microgels were studied through atomic force microscopy (AFM). Using tapping mode, the microgels were found to have a narrow size distribution with a diameter of approximately 275 nm (Figure 1). The emulsion polymerization proceeded using 20% styrene and 80% 2-vinylpyridine because previous studies by Curtis *et al.* showed that this ratio was optimal for pH-

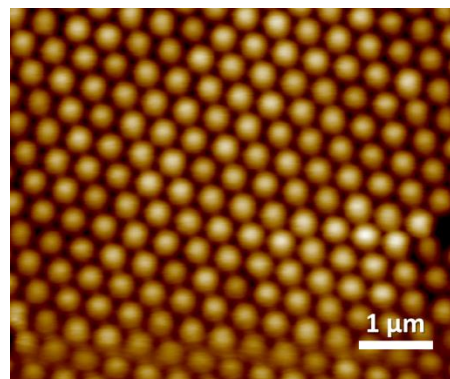


Figure 1. AFM image of $\text{PS}_{20}\text{P2VP}_{80}$ microgels acquired using the tapping mode setting.

swelling and contracting over several acid-base titration cycles.¹ As the pH is decreased, the basic nitrogen on the pyridyl groups become protonated, causing the microgels to swell. The DVB crosslinker holds the microgel together, allowing it to swell and contract without losing its form. A graduate student in the Emory group previously found that the diameter of the microgels under acidic conditions could increase up to approximately 720 nm, on average, and that the swelling occurred in all three dimensions.⁶ These sterically stabilized microgel beads were found to act as a scaffold for metal NP adsorption to their surface. Anchoring SERS-active metal NPs on a polymer substrate increases their stability and sensitivity and improves reproducibility in SERS studies.

The PS₂₀P2VP₈₀ microgels were loaded with Au NP seeds using potassium tetrachloroaurate(III) and DMAB reducing agent. In the first step of the reaction, Au³⁺ ions were electrostatically loaded onto the microgels, where the addition of DMAB reduced them to Au(0) NP seeds on the microgel surface. During this process, the gold anions coordinated to the basic nitrogen on the pyridyl groups within the random copolymer microgel beads. Upon analysis of the STEM image, the diameter of each NP was found to be approximately 15 nm, and the interparticle distance was calculated to be 10 nm on average (Figure 2).⁶

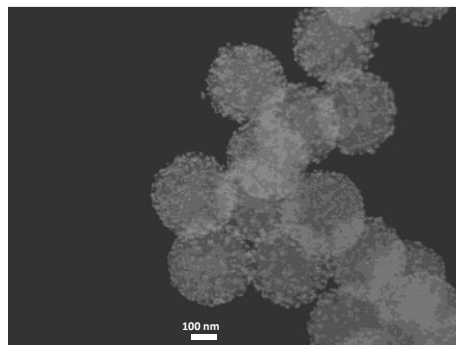


Figure 2. SEM image of AuNP seeds adsorbed to the surface of the PS₂₀P2VP₈₀ microgels. The diameter of each AuNP was measured to be 15 nm, and the AuNP interparticle distance was calculated to be 10 nm.

Another addition of potassium tetrachloroaurate(III) along with the weak reducing agent, hydroxylamine hydrochloride, promoted Au growth on the previously adsorbed Au seeds rather than new nucleation. These Au@AuNP-PS₂₀P2VP₈₀ microgels were the intended composite material for SERS spectroscopic signal enhancement in this work. The Au@AuNP-PS₂₀P2VP₈₀

microgels were studied using STEM to confirm their morphology and EDS to confirm elemental composition. The STEM data revealed that the AuNP-seeds on the surface of the microgel beads had grown from ~ 15 nm to approximately 35 nm while the interparticle distance decreased from 10 nm to 0.5 nm (Figure 3).⁶ This decrease in interparticle distance is known to increase the

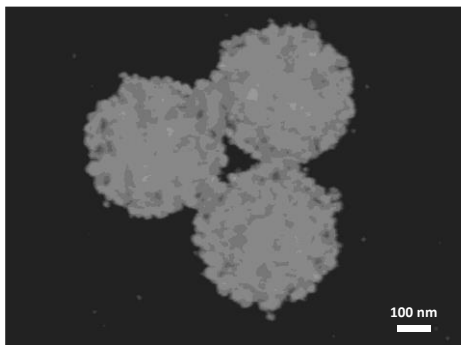


Figure 3. SEM image of Au@AuNP-PS₂₀P2VP₈₀ microgels. The NP diameter was found to be 35 nm, and the interparticle distance between each NP cluster was calculated to be 0.5 nm. The scale bar represents 100 nm.

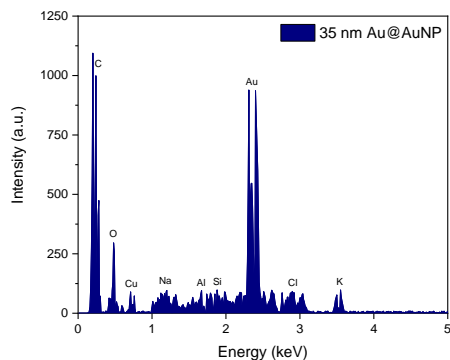


Figure 4. EDS spectrum of the Au@AuNP-PS₂₀P2VP₈₀ microgels. The largest peaks in the spectrum are due to the presence of C and Au.

SERS-activity and can be controlled further through tuning the sample pH, and consequently the diameter of the microgels. The EDS spectrum confirmed the elemental composition, with large peaks corresponding to C and Au (Figure 4).⁶ The signal from C atoms arose from their presence in the random PS₂₀P2VP₈₀ copolymer. The large signal from Au was due to the NPs grown on the surface of the microgel beads. The EDS spectrum confirmed the assumption that the NPs in the STEM image were AuNPs.

The Au@AuNP-PS₂₀P2VP₈₀ microgels were then used for SERS enhancement studies by Raman microscopy. A 1 μ M crystal violet (CV) solution was made by dissolving CV powder in ethanol. This CV solution (20 μ L) was mixed with Au@AuNP-PS₂₀P2VP₈₀ microgels (200 μ L)

for 30 min before being deposited on a glass coverslip for SERS spectroscopy. The sample was imaged under the Raman microscope and a spectrum was acquired (Figure 5). The CV peak at 1177 cm^{-1} was of particular interest due to its intensity and impressive signal-to-noise ratio; the intensity of this peak was mapped across a rectangular area of the sample image (Figure 6). The

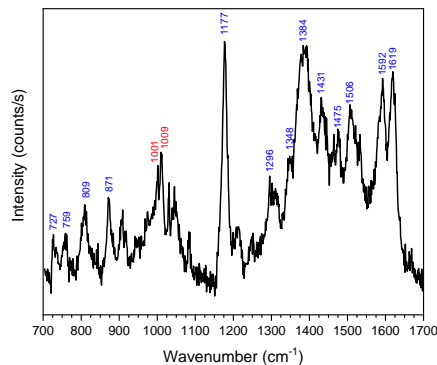


Figure 5. Raman spectrum of CV in ethanol ($1 \mu\text{M}$, $20 \mu\text{L}$) mixed with Au@AuNP-PS₂₀P2VP₈₀ microgels ($200 \mu\text{L}$). Blue peaks are CV, red peaks are from the microgels. Spectrum was acquired using a He-Ne laser at a power of $1,2000 \mu\text{W}/\mu\text{m}^2$ for an integration time of 1 s.

signal-to-noise ratio of the vibrational peaks in the Raman spectrum were phenomenal considering the use of a low concentration CV solution ($1 \mu\text{M}$), using ten times more microgel solution than CV solution in the volume of sample mixture, as well as acquiring the image using relatively low power from the He-Ne laser with only a 1 s integration time (Figure 6A). When mapping the 1177 cm^{-1} peak intensity across the sample image, the resolution of the map was limited by the spot size of the laser. In the rectangular intensity map, the laser hit the

sample 175 times, creating a 5-pixel by 35-pixel raster image (Figure 6B). Brighter yellow pixels indicate a higher intensity of the peak signal. From this intensity map, it was found that the SERS signal was localized on the AuNPs. The localized surface plasmon resonance of each AuNP enhanced the Raman signal intensity through the coherent oscillation of these surface plasmons resonant with the wavelength of the 633 nm He-Ne laser excitation source.

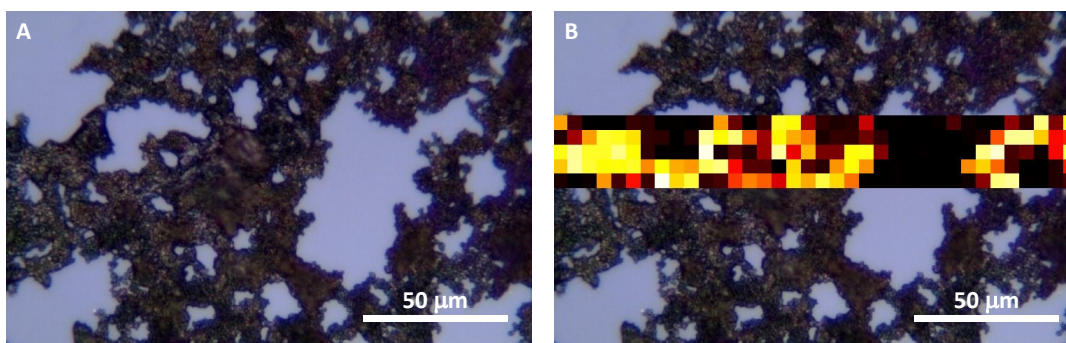
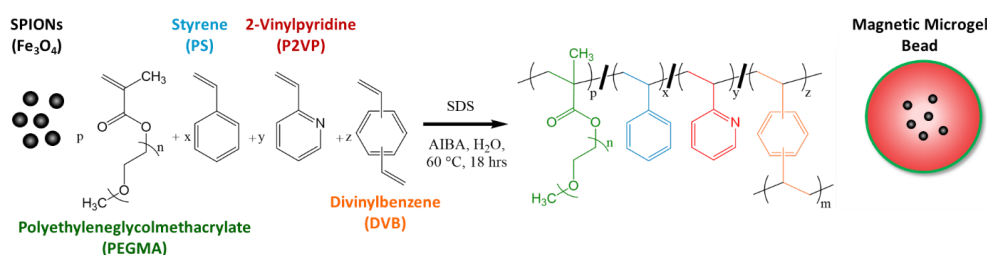


Figure 6. Raman microscope image of a CV and Au@AuNP-PS₂₀P2VP₈₀ microgel mixture. A) depicts the sample, and B) depicts the 1177 cm^{-1} peak intensity from Figure 5 mapped across a 5×35 -pixel rectangle of the sample.

After proving the SERS enhancement capabilities of the Au@AuNP-PS₂₀P2VP₈₀ microgel system, the next goal was to introduce a magnetic component to the microgels to create a NP-based detection system that could be extracted magnetically from a sample matrix. SPIONs were synthesized and dispersed in the SDS surfactant solution to create an initial emulsion of SPIONs, which was predicted to improve encapsulation efficiency. The emulsion polymerization theoretically created a PS₂₀P2VP₈₀ microgel with SPIONs encapsulated in the core of the polymer beads (Scheme 1).



Scheme 1. Magnetite encapsulation into PS₂₀P2VP₈₀ microgel beads.

Before encapsulation attempts, the SPIONs were characterized by powder XRD and Raman spectroscopy. The XRD pattern of the SPION sample matched with the Fe₃O₄ reference pattern, confirming the identity of the SPION crystals (Figure 7). The diameter of the crystal lattice was calculated to be 6.3 nm using Bragg's Law. The optimal diameter of Fe₃O₄ crystals is 7-10 nm because it has been reported that this size range is good for minimizing the effect of moment reduction.⁵ The diameter of the experimentally-produced magnetite was 0.7 nm short of this optimal range, but still close in size. The Raman spectrum of the Fe₃O₄ sample showed a large peak at 674 cm⁻¹, which is redshifted 4 wavenumbers from the literature value of 670 cm⁻¹ for magnetite, but is still within a close range of the expected peak location (Figure 8).⁷

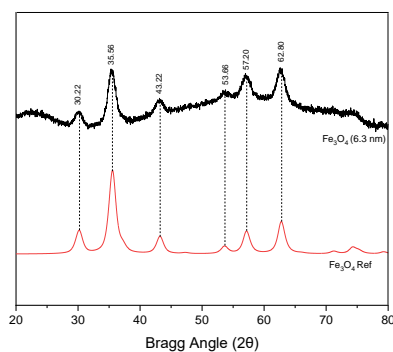


Figure 7. Powder XRD pattern of Fe₃O₄ crystals.

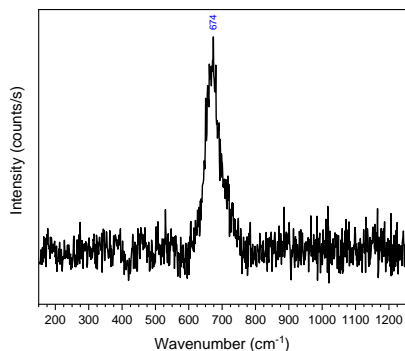


Figure 8. Raman spectrum of the Fe_3O_4 sample.

The magnetite-encapsulated microgels were purified by magnetic extraction and studied using an optical microscope. The sample was found to have a large size distribution of microgel particles (Figure 9). This is in stark contrast to the uniform size of the nonmagnetic $PS_{20}P_{2VP_{80}}$ microgels studied by AFM (Figure 1). It was found that there were three distinct microgel size groups. The first group was the ‘mega’ particles with diameters of 10 microns, approximately. A small particle group existed where each structure was less than one micron in diameter. The mid-sized particles appeared to be between one and five microns and were susceptible to an applied magnetic field. When the optical image was acquired, the sample solution was suspended between two coverslips to delay the evaporation process. A neodymium magnet was passed back and forth along the sample stage, where the mid-

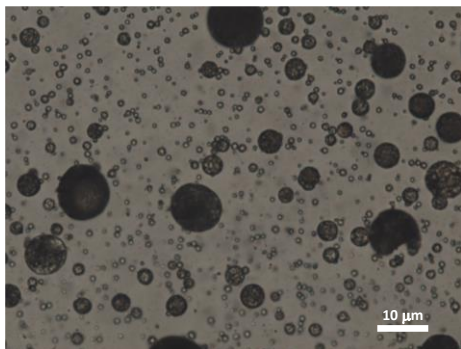


Figure 9. Optical microscope image of magnetite-encapsulated $PS_{20}P_{2VP_{80}}$ microgels. Image was acquired at 80x magnification.

sized particles reacted by rocking back and forth in sync with the magnet. This showed that, in at least one size population, magnetite was able to be encapsulated in $PS_{20}P_{2VP_{80}}$ microgels. Future work must be done to improve the encapsulation methods to fix the large size distribution of microgels created, as well as the uneven loading of magnetite into their cores.

4. Conclusions

A pH-swelling random copolymer of PS₂₀P2VP₈₀ was synthesized, characterized, and found to have a diameter of 275 nm at basic pH levels. Using this polymer substrate, AuNP seeds were loaded onto the surface where they acted as anchors for another addition of AuNPs to grow on. It was demonstrated that the AuNPs could grow to 35 nm on the microgel surface while maintaining the microgel's ability to swell and de-swell in response to changes in pH.⁶ These Au@AuNP-PS₂₀P2VP₈₀ microgels were used to enhance the Raman signal through the SERS effect. A magnetic component was attempted to be incorporated into the multifunctional microgel system but was found to have an uneven encapsulation efficiency over the different microgel sizes in the sample solution. Future work will be done to improve this magnetite-encapsulation procedure so that AuNPs may be grown on the surface of PS₂₀P2VP₈₀ microgels with SPIONs in their cores.

References

- (1) Curtis, T.; Taylor, A. K.; Alden, S. E.; Swanson, C.; Lo, J.; Knight, L.; Silva, A.; Gates, B. D.; Emory, S. R.; Rider, D. A. Synthesis and Characterization of Tunable, PH-Responsive Nanoparticle–Microgel Composites for Surface-Enhanced Raman Scattering Detection. *ACS Omega* **2018**, *3* (9), 10572–10588. <https://doi.org/10.1021/acsomega.8b01561>.
- (2) Eustis, S.; El-Sayed, M. A. Why Gold Nanoparticles Are More Precious than Pretty Gold: Noble Metal Surface Plasmon Resonance and Its Enhancement of the Radiative and Nonradiative Properties of Nanocrystals of Different Shapes. *Chem Soc Rev* **2006**, *35* (3), 209–217. <https://doi.org/10.1039/B514191E>.
- (3) Moskovits, M. Surface-Enhanced Spectroscopy. *Rev. Mod. Phys.* **1985**, *57* (3), 783–826. <https://doi.org/10.1103/RevModPhys.57.783>.
- (4) Górka, W.; Kuciel, T.; Nalepa, P.; Lachowicz, D.; Zapotoczny, S.; Szuwarzyński, M. Homogeneous Embedding of Magnetic Nanoparticles into Polymer Brushes during Simultaneous Surface-Initiated Polymerization. *Nanomaterials* **2019**, *9* (3), 456. <https://doi.org/10.3390/nano9030456>.
- (5) Xu, Z.; Shen, C.; Hou, Y.; Gao, H.; Sun, S. Oleylamine as Both Reducing Agent and Stabilizer in a Facile Synthesis of Magnetite Nanoparticles. *Chem. Mater.* **2009**, *21*, 1778–1780.
- (6) Silva, A. Multifunctional Microgels for Nanoparticle-Based Detection Methodologies.
- (7) Slavov, L.; Abrashev, M. V.; Merodiiska, T.; Gelev, Ch.; Vandenberghe, R. E.; Markova-Deneva, I.; Nedkov, I. Raman Spectroscopy Investigation of Magnetite Nanoparticles in Ferrofluids. *J. Magn. Magn. Mater.* **2010**, *322* (14), 1904–1911. <https://doi.org/10.1016/j.jmmm.2010.01.005>.